# Self Pumping Paper Based Formic Acid Fuel Cell

**Anand Sagar**

A Thesis Submitted in Partial Fulfillment of the Requirements

for the Degree of Master of Technology

**Adviser- Dr.Kirti Chandra Sahu**

**Dr.Vinod Janardhanan**

भारतीय प्रौद्योगिकी संस्थान हैदराबाद
Indian Institute of Technology Hyderabad

**Department Chemical Engineering**

**Indian Institute Of Technology Hyderabad**

**June,2015**

# Declaration

I declare that this written submission represents my ideas in my own words, and where ideas or words of others have been included, I have adequately cited and referenced the original sources. I also declare that I have adhered to all principles of academic honesty and integrity and have not misrepresented or fabricated or falsified any idea/data/fact/source in my submission. I understand that any violation of the above will be a cause for disciplinary action by the Institute and can also evoke penal action from the sources that have thus not been properly cited, or from whom proper permission has not been taken when needed.

Anand Sagar.

(Signature)

(Anand Sagar)

CH13M1001

(Roll No.)

# Approval Sheet

This Thesis entitled 'Self Pumping Paper Based Formic Acid Fuel Cell' by Anand Sagar is approved for the degree of Master of Technology from IIT Hyderabad

(Dr.M.Deepa) Examiner
Dept. of Chemistry
IITH

(Dr.Narasimha Mangadoddy) Examiner
Dept. of Chem Eng
IITH

(Dr.Kirti Chandra Sahu) Adviser
Dept. of Chem Eng
IITH

(Dr.Vinod Janardhanan) Co-Adviser
Dept. of Chem Eng
IITH

# Acknowledgment

The work done by me for my M.Tech degree would never have been possible without the support of a number of people. I am indebted to Dr.Kirti Chandra Sahu, my supervisor for his continuous support and guidance at every stage of my work. I have learnt a lot from him which made me understand, what research is all about which helped me grow as a budding researcher. I am also very grateful to have Dr.Vinod Janardhanan and Dr.M.Deepa as my co-advisors, who helped me a lot building my concepts in my research area, on various theoretical and experimental aspects. Under their mentorship only, I was able to inculcate the ideas into work.

I would like to thank the Chemistry department of IIT,Hyderabad specially the 'Electrochemistry Lab' people, supervised by Dr.M.Deepa for helping me perform my experiments at their research facility. My sincere thanks also extends to Dr.M.Ramji, Mechanical Engineering Dept. for providing me work facilities at Central Workshop and Dr.Chandra Shekar Sharma for utilizing the facilities at Nano Lab in our department.

I would also like to acknowledge my colleague Sweta Lal for her support in various stages of my work. Naresh Kumar Pendyala and Mukkabla Radha were also of great help introducing me to the lab setup, I thank them for this. I would also like to show my sincere gratitude to all the faculty members of Chemical Engg Dept. and my fellow mates for showing confidence and support to me.

In addition to the excellent professional mentorship and guidance I have received, my deepest gratitude goes to my family for their unending patience and belief in me over the past years. My mother, father and my sister have been a constant source of support for me at all times.

# Dedication

I dedicate this to my parents.

**Abstract**

Fuel cells have been a source of green energy and is rapidly gaining applications in various fields. Laminar flow fuel cells are special type of fuel cell in which the oxidant and the fuel flow in parallel, mixed with the electrolyte, which substancially reduces losses due to mixing.

This work focuses on the fabrication of paper based laminar flow fuel cells with a slit in between the two electrode areas to prevent further crossover. The capillary action of Whatman filter paper has been used which makes the cell self pumping hence reducing the power requirements. Formic acid is used as fuel and potassium permagnate is used as oxidant. Concentration of the fuel has been varied and corresponding change in polarization curves, potentiometry, impedance curves has been studied using Autolab. The proposed cell can be used as a lateral flow in small diagnostic devices, which requires low power for their operation.

# List of Figures

# List of Tables

# Contents

# 1 Introduction

## 1.1 Overview: Fuel cells

Fuel cell is an electrochemical device which utilizes the chemical kinetics of the reactions taking place at the respective electrodes, i.e anode and cathode to convert the chemical potential energy into electrical energy. However, it works on the same principle as that of conventional batteries, it differs in terms of the fuel being used continuously to produce electricity and hence can be used as a constant source of energy without having the drawbacks of charging and discharging. It also benefits over the internal combustion(IC) engines widely being used in automobiles, in a way that it reduces the effort of combustion of the fuel being used which makes it a more efficient source of energy.

Fuel cells can use fuels in gaseous as well as liquid state which makes it fuel-flexible. The electrolyte used in the fuel cell can also be selected based on the applications of the cell. It can be of various structures and in various phases like molten state in molten carbonate fuel cell(MCFC)[10], solid in polymer electrolyte membrane fuel cell(PEMFC) etc. No moving parts are present in the fuel cell, which provides stability. The absence of mechanical components in the cell also makes it a silent device and requires low maintenance. The air polluting components are also eliminated in the fuel cell as compared to other energy sources, making it a green source of energy like solar, wind, biofuel. The kinetics of the reactions at the respective electrodes are of prime importance for a fuel cell design, which decides the losses in the cell and the overall performance making the cell more selective. The design and the fabrication of the cell is highly based on its uses, like a miniaturized microfluidic device for a low energy device to a giant structured cell for providing electricity to a building. So, overall the fuel cells can be assumed to be highly selective, flexible and cleaner device so as to be a prominent replacement to most of the conventional power sources being used recently.

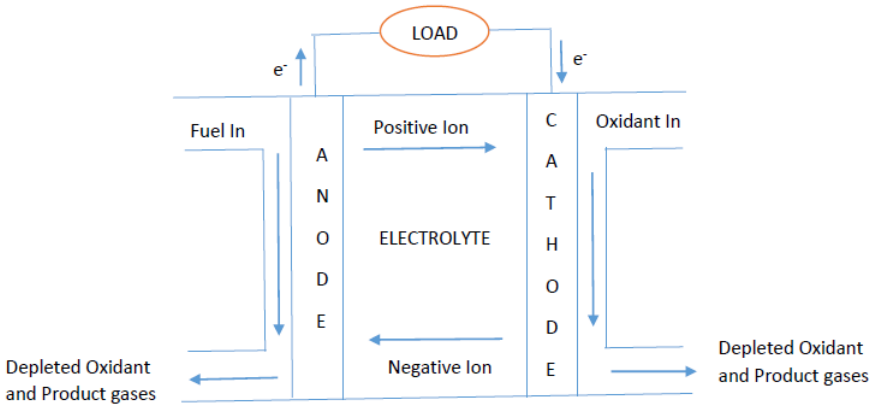


Figure 1: Schematic of a fuel cell

Figure 1 describes the general schematic of a fuel cell.

## 1.2 Performance of a fuel cell

The performance of a fuel cell can be decided based on how much the actual cell potential deviates from the equilibrium potential, which can be considered as the base state. The ideal equilibrium potential is given by Nernst equation, which relates the standard potential of the cell at given temperature and pressure conditions to the ideal state equilibrium potential. The actual performance of the cell is decided by the actual voltage across the cell, that is ideally less than the equilibrium value due to various kinds of losses like activation losses, ohmic losses, mass transfer losses, mixed potential losses etc. These losses are well explained for the experiment under the impedance study part, in chapter 3. Figure 2 is a typical polarization curve for a fuel cell, which is a plot between current density and the cell voltage. It clearly demarcates the regions of various losses occurring inside the cell.

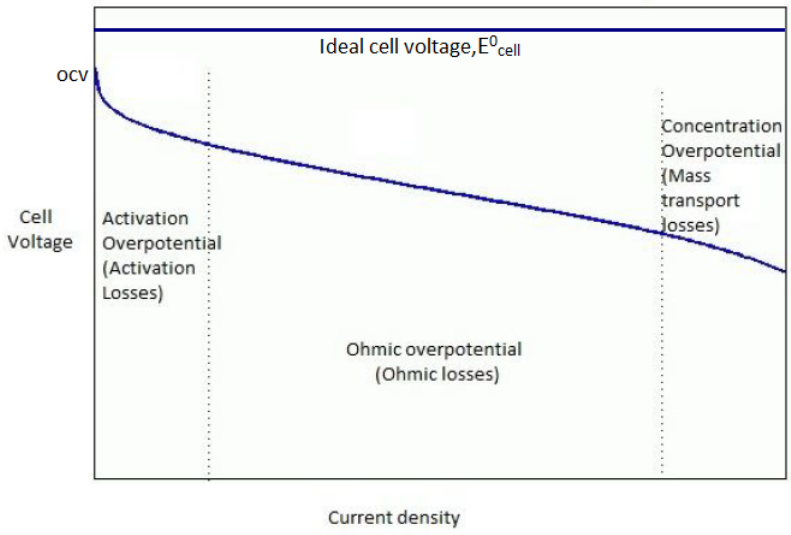


Figure 2: Typical polarization curve of a fuel cell

## 1.3 Laminar flow fuel cell

The fuel cell concept was introduced long back and various types of fuel cells based on the applications were functioning like Polymer electrolyte membrane fuel cell(PEMFC), Phosphoric acid fuel cell, Solid oxide fuel cell, Alkaline fuel cell etc. Ferrigno et al.(2002)[12] for the first time introduced the concept of laminar flow fuel cell, which was based on exploiting the concept of laminar flow of fluids. It was demonstrated that at low reynold's no(Re), if two fluids are flowing then eliminating the convecting mixing between the fluids, they can move parallely with only diffusive mixing at the interface. This work suggested the elimination of membrane from the fuel cell, which can drastically reduce the overall cost of the cell. They have reported the OCV of 1.52V with the use of redox couples at the electrodes. However, the fuel utilization was found to be only 0.1% due to mass transport limitations. Choban et al.(2005)[7] also reported in their work of eliminating issues like fuel crossover, cathode flooding, anode dryout by use of laminar flow fuel cell. They have operated the fuel cell under various conditions of alkaline, acidic, mixed media and studied the media-flexibility of the cell. It was concluded that while

changing the fuel or the oxidant concentration, there is no change required in the fuel cell.

## 1.4 Effect of different fuel, oxidant and electrolyte

As the reactions involved at the electrodes are solely dependent on the fuel and oxidant, the cell voltage obtained is different for different fuel and oxidants based on their respective equilibrium cell potentials. Choban et al.(2004)[6] first studied the performance of the fuel cell on the variation of oxidant. They used two different oxidants 0.144M $KMnO_4$ in 0.5M $H_2SO_4$ and oxygen saturated in 0.5M $H_2SO_4$ with 2.1M HCOOH as common fuel. They for the first time tried to mix a proton source, which is $H_2SO_4$ at both the anode and cathode streams. This increased the proton conductance by availability of protons near the cathode. It was noted that the nature of the polarization and the power density curve were same for the two cases. However, for $KMnO_4$ system the OCV and maximum power density came to be on higher side. This trend can be attributed to the higher equilibrium potential of $KMnO_4$ reduction as compared to $O_2$. Similar work was done by López et al.(2011)[24] using $KMnO_4$ as an oxidant in a silicon based micro laminar flow fuel cell which gave a power density of 26mW$cm^{-2}$. They also introduced a bridge in between the two anodic and cathodic microchannels of the cell, which drastically reduces the mixing all along the cell producing a higher power and current density.

Jayashree et al.(2005)[18] proposed an air-breathing cathode which can directly inhale oxygen in form of air from the environment. The mass transfer limitations offered by the dissolved oxygen in a laminar flow fuel cell was reduced by the use of a porous air-exposed gas diffusion electrode(GDE) as the cathode which takes oxygen directly from air. A power density of 26mW$cm^{-2}$ and a current density of 130mA$cm^{-2}$ at 1M HCOOH as fuel was obtained, which was quiet higher compared to dissolved $O_2$ being used as an oxidant. Further Kjeang et al.(2007)[21] also exploits the higher reduction potential of $H_2O_2$ which is 1.776V and uses it

as an oxidant to gain power density upto 26mW$cm^{-2}$ and current density of 150mA$cm^{-2}$ with formic acid as the fuel at room temperature. Braff et al.(2013)[2] in their work showed the use of aqueous $Br_2$ as an oxidant with gaseous $H_2$ as fuel on anode side. They have used the fast, reversible kinetics of the reactions taking place at electrodes to overcome the activation losses leading to a power density as high as 795mW$cm^{-2}$.

Brushett et al.(2009)[3] have done a study on an air-breathing laminar flow fuel cell with five different fuels namely methanol, ethanol, formic acid, hydrazine and sodium borohydride under different media with the similar catalyst loading on anode and cathode in each case. It was observed that in acidic media, formic acid shows better performance as compared to methanol and ethanol. However, the electrode kinetics was seen higher in alkaline medium for methanol,ethanol and sodium borohydride, but not for hydrazine and formic acid. Hydrazine and sodium borohydride was found to be showing maximum power densities of 80mW$cm^{-2}$ and 101mW$cm^{-2}$ respectively. Mota et al.(2012)[27] have used yet another redox couple with Borohydride($BH_4^-$) as fuel and Cerium ammonium nitrate as an oxidant producing a power density of around 250mW$cm^{-2}$m in a membraneless microfluidic fuel cell eliminating the anode poisoning issues due to CO impurities.

## 1.5 Effect of cell geometry and electrode surface

The design of the fuel cell plays a major role in the working of the cell. Chang et al.(2006)[4] have used a Y-shaped microchannel for the numerical analysis of their laminar flow fuel cell. The fuel and the oxidant after entering through the inlets, flow parallel without any membrane in between. The role of the geometry of the cell on the cell performance was studied and it was found that for a fixed aspect ratio and volumetric flow rate, lower cross-section area gives better performance of the cell, whereas for a constant cross-section area higher aspect ratio gives better

results. Similar numerical work was done by Park et al.(2009)[28] with a H-shaped cross-section. A small passage between the anode and the cathode was thus provided in this type of geometry, which reduces the mixing of the two fluids on anode and cathode side. As a result it was found that when the mixing region was reduced by 20%, the fuel crossover decreased to ten times as compared to the usual rectangular cross-section case. The fuel utilization was also observed to be increased by 8% for their case. Rafael et al.(2013)[14] also presented their finite element results based on various geometries of rectangular shape, cylindrical shape and star shaped cell. Keeping the volume-to-length ratio same in all the cases, it was noted that the fuel utilization was increased upto 89% and 68.2% in star and cylindrical shaped geometries as compared to 42.4% in rectangular case. The net current density was also observed to be higher by 1200% and 400% for star and cylindrical shape as compared to the rectangular one.

The nature of the electrode surface also decides the performance of the cell, as the reactions taking place at the respective electrodes directly depends on this. Kjeang et al.(2008)[22] included the flow-through porous electrodes concept in their work. This concept uses the full depth of the porous electrode structure and the overall active area is drastically increased. The mass transfer from the bulk to the desired active area is highly increased as a result. The fuel utilization observed was almost 100% with a power density of nearly 131mW$cm^{-2}$. Ha et al.(2014)[15] in their study incorporated the grooved electrode surface in their laminar flow based fuel cell. The grooved electrode present adds a secondary flow replenishing the reaction depletion zone.The maximum power density was observed to be increased by 13.93% compared to the planar electrodes.

## 1.6 Paper based laminar flow fuel cell

Fraiwan et al.(2013)[13] presented a paper based microbial fuel cell which included micro-fabricated paper chambers and a paper based proton exchange membrane. The ease of use,

better portability and low production cost are the advantages of such kind of cell. The main feature of the paper based proton exchange membrane lies in its development, which is done by soaking the paper in sodium polystyrene sulfonate, which also works as an electrolyte and is capable of conducting ions. The induced hydrophobic property of the paper reduces the crossover by obstructing the flow of water and thereby allow protons to pass through at a greater extent resulting in higher efficiency. Arun et al.(2014)[1] have worked on a self pumping air-breathing paper based laminar flow fuel cell. They have used the pencil stroked graphite as the electrodes for their cell, which makes the paper-electrode area hydrophobic and thus restricts the flow of fuel near the electrode. The transport of protons is increased as a result which is further supported by the non-ordered complex fibre network of the paper. The observed power density was 32mW$cm^{-2}$ for a period of nearly 1000 minutes. Esquivel et al.(2014)[11] have also reported a similar kind of work to produce power for lateral flow devices with methanol as fuel on paper-based fuel cell. They have also exploited the capillary action of the paper for pumping of fuel and oxidant on to the cell. Here, the paper behaves as a channel, reagent storage as well as the waste sink. They have reduced the crossover issues by providing a slit on the paper, which separates the two flows on anode and cathode side. They have reported the maximum power density to be 4.4mW$cm^{-2}$ at a current density of 22.5mA$cm^{-2}$ with 4.0M $CH_3OH$ as fuel and 2.0M KOH as an oxidant.

## 1.7 Study objectives

The present work is based on the objectives of fabrication of a cost effective, energy efficient, portable and miniaturized lateral flow device which can be used as a diagnostic device in future. The principle of the work lies on the laminar flow fuel cell concept. The cell is fabricated based on the self pumping capillary action of the Whatman filter paper, which makes it energy efficient and self actuating device. A unique design of Y-shaped structure with a slit in between has been inculcated to reduce crossover losses further in the cell. The design and fabrication part of the cell is well explained in chapter-3. Various characteristic tests have also been performed on the fabricated cell which are well explained in the chapter-3 and chapter-4 respectively.

Table 1 below summaries recent works on Formic acid fuel cell with different oxidants and electrode conditions.

Table 1: Summary of important works done on formic acid fuel cell

| **Anode** | **Cathode** | **Temp (K)** | **Fuel** | **Oxidant** | **Flow rate** ($mlmin^{-1}$) | **OCV(V)** | $P_{max}(mWcm^{-2})$ | $I_{max}(mAcm^{-2})$ | **Ref.** |
|---|---|---|---|---|---|---|---|---|---|
| Pd black ($10mgcm^{-2}$) | Pt black ($2mgcm^{-2}$) | 298 | HCOOH | 0.5M $H_2SO_4$ | | 0.94 | 26 | 125 | [20] |
| Pd/C | Pt/C | 298 | 0.5 M HCOOH in 0.5M $H_2SO_4$ | Dissolved $O_2$ in 0.5M $H_2SO_4$ | 0.2 | 0.9 | 5.3 | 11.5 | [9] |
| Pd/V XC-72 | Pt/V XC-72 | 298 | 0.5M HCOOH | Dissolved $O_2$ in $H_2SO_4$ | 0.2 | 0.98 | 3 | 7.5 | [26] |
| Pd black | Pt black | 298 | 1 M HCOOH in 0.5M $H_2SO_4$ | Dissolved $O_2$ in 0.5M $H_2SO_4$ | 0.3 | 0.9 | 26 | 130 | [19] |
| Pd black($1mgcm^{-2}$) | Pt black($1mgcm^{-2}$) | 298 | 5M HCOOH | Air breathing | | 0.64 | 19.6 | 100 | [16] |
| PdPt/C | Pt black | 298 | 5M HCOOH | Air breathing | | 0.77 | 20 | 4.8 | [17] |
| Pt/C | Pt black | 298 | 5M HCOOH | Air breathing | | 0.62 | 35 | 6.3 | [17] |
| Pd/C | Pt black | 298 | 5M HCOOH | Air breathing | | 0.77 | 65 | 1.2 | [17] |
| PdCo2/MWCNT | Pt black | 298 | 0.5M HCOOH | Dissolved $O_2$ in 0.5M $H_2SO_4$ | 0.485 | 0.89 | 1.5 | 4.6 | [25] |
| Pd/MWCNT | Pt black | 298 | 0.5M HCOOH | Dissolved $O_2$ in 0.5M $H_2SO_4$ | 0.485 | 0.82 | 0.85 | 2.9 | [25] |
| PdCo1/MWCNT | Pt black | 298 | 0.5M HCOOH | Dissolved $O_2$ in 0.5M $H_2SO_4$ | 0.485 | 0.9 | 1.75 | 5.9 | [25] |
| Pt black | Pt black | 298 | 2.1M HCOOH in 0.5M $H_2SO_4$ | 0.144M $KMnO_4$ in 0.5M $H_2SO_4$ | 0.5 | 1.15 | 2.5 | 8 | [5] |
| Pt electrodes | Pt electrodes | 298 | 2M HCOOH | 0.144M $KMnO_4$ in 0.5M $H_2SO_4$ | 0.5 | 1 | 0.7 | 2.5 | [31] |
| Plain graphite | Plain graphite | 298 | 10M HCOOH in 4M $H_2SO_4$ | 1M $KMnO_4$ in 4M $H_2SO_4$ | | 1 | 2.6 | 3.61 | This work |

# 2 Experimental setup

## 2.1 Overview

The fuel cell being described here is a type of laminar flow fuel cell with self pumping nature. External power is required in most of the cells to pump the fuel and the oxidant in the fuel channel and oxidant channel respectively. The capillary action of 'Whatman filter paper' has been used to pump fuel and oxidants in this system which eliminates the power requirement for fuel pumping onto the cell. That is why, this fuel cell is termed as self pumping. The pores present in the filter paper helps in flow of the solution and also maintains laminar nature of flow because of the very smaller flow rates. This laminar nature of the two flows help them move parallely and hence reduce mixing other than diffusion of protons released on anode at the interface.

## 2.2 Design and fabrication

The cell is designed in a Y-shaped structure cut on a 'Whatman filter paper'. The fuel Formic acid(HCOOH) and the oxidant($KMnO_4$) enters through the two extreme wings of the Y-shaped structure. A slit of length 3.5cm and width 4mm (optimized) is made at the entrance of the cell, where the two fluid enters the cell. The slit is being provided here to reduce the probability of mixing of the fuel and the oxidant, hence lowering the crossover.

The graphite electrodes on both the sides of area $0.35cm^2$ is made in contact with the filter paper which in turn comes in contact with the fluid flowing at the two electrodes. The oxidation and reduction reaction takes places at anode and cathode respectively producing a voltage difference between them which correspondingly produces a current that can be measured through the wires attached at both the electrodes. An absorbent pad made of foam is attached at the end of the cell which behaves as the sink for absorbing the flow and making the process

continuous. Figure 3 describes the design of the cell.

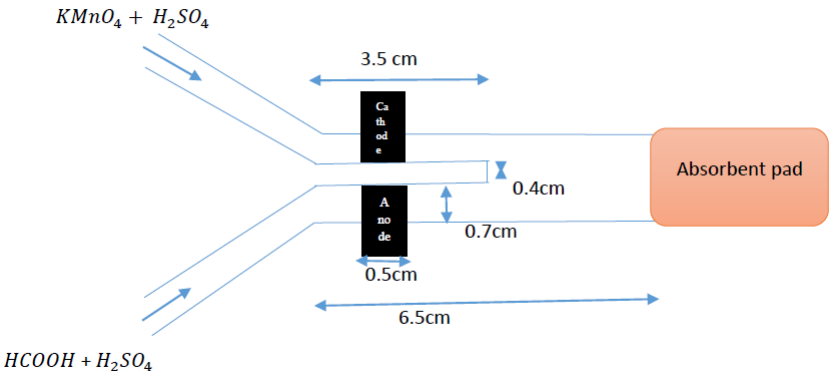


Figure 3: Design of the experimental fuel cell

## 2.3 Components of the cell

The various components of the cell are as below

- Fuel - The fuel used in the system is formic acid(HCOOH). HCOOH is a liquid fuel which can work at the operating temperature of $25^0$C i.e at room temperature with reasonably good electro kinetics. The advantage of HCOOH being used as a fuel is that it is portable and cost effective. It is also non toxic as compared to other fuels like methanol. The HCOOH of various concentrations ranging from 6-12M are mixed with 4M $H_2SO_4$ and is fed as fuel on the anode side of the cell.

- Oxidant - Various oxidants has been used in the conventional fuel cells with $O_2$ being used widely. However, we chose KMn$O_4$ as an oxidant for this system because of its reduction potential being 1.49V as compared to 1.23V that of $O_2$. 1M KMn$O_4$ solution was mixed with 4M $H_2SO_4$ and fed as oxidant on the cathode side. The two solutions needs to be mixed properly before use to prevent coagulation on the flow pathway. The concentration of KMn$O_4$ was varied but no significant changes were observed in the system.

- Electrolyte - The electrolyte plays a major role in transportation of ions from anode side to cathode side for the working of the cell. $H_2SO_4$ has been used as an electrolyte in the system, which is mixed in both fuel and oxidant for better transportation of protons.

- Anode - Graphite sheet of area $0.35cm^2$ and thickness 1.3mm is being used as electrode in the anode side. The electrode is placed below the cell system in contact with the filter paper. So, when the fuel flows through the filter paper it touches the upper side of the graphite electrode where oxidation of the fuel takes place. No catalyst has been used so far on the electrode as we were able to gain the current density required for the cell application purpose. The external tip of the electrode coming out of the system is attached with crocodile clip which connects it to the external load.

- Cathode - Graphite sheet of area $0.35cm^2$ and thickness 1.3mm is being used as electrode in the cathode side as well. The electrode is placed above the cell system in contact with the filter paper. So, when the fuel flows through the filter paper it touches the lower portion of the graphite electrode where oxidation of the fuel takes place. No separate current collector is used as graphite sheet is itself conducting and acts both as current collector and electrode. Here also, no catalyst has been used so far on the electrode as we were able to gain the current density required for the cell application purpose. The external tip of the electrode coming out of the system is attached with crocodile clip which connects it to the external load.

- Slit - A unique design of slit is being introduced, which works well with the system. Slit is a hollow rectangular structure made at the entrance of the cell, which effectively stops the mixing of the fuel and the oxidant before their oxidation and reduction respectively, hence eliminating the crossover issues. The slit width is optimized to 4mm with a length

of 3.5cm. Although, a bit higher length of the slit increases the diffusional length for transportation of proton from anode to cathode side, it compensates with the crossover being minimized.

- Channel - The flow of fuel and oxidant and the diffusion mixing at the interface all takes place on the filter paper channel which acts as a supporting media for transportation of protons and the flow. The micro pores present in the filter paper enables the flow through it. The total channel length excluding the slit length is 3cm.

- Absorbent pad - The flow channel of the cell is provided with an absorbent pad at the end of the channel. It acts as a sink for the flowing fluid by absorbing them and hence making the process continuous eliminating the flooding issues. The pad is made of sponge like material for better absorption.

## 2.4 Working Mechanism

The cell described above shown in Figure 4 works on the principle of laminar flow cells with fuel and oxidant flowing in the laminar flow regime. The fuel comprising of HCOOH and $H_2SO_4$ gets pumped through the anode side channel by the capillary action of the filter paper. It then travels to the electrode on the anode side and oxidation of HCOOH takes place at this site. As a result protons are released at the anode which travels to the cathode side flowing through the electrolyte ($H_2SO_4$) medium. Similarly, the oxidant comprising of $KMnO_4$ and $H_2SO_4$ enters the cell through the channel on the cathode side and flows to cathode side electrode where reduction of $KMnO_4$ takes place. The electrons released at the anode side travels through the outer circuit and comes on cathode which accounts in the reduction reaction at cathode. $H_2O$ is formed as a by-product at this site. The slit used helps in dividing the two flows and hence prevents mixing at any point. Both the fluids continuously flow through the filter paper based

channel and gets absorbed at the absorbent pad making the process continuous. The reactions involved are

Anode: $HCOOH \rightarrow CO_2 + 2H^+ + 2e^-$ $E^0 = -0.25V$ [32]

Cathode: $MnO_4{}^- + 8H^+ + 5e^- \rightarrow Mn^{+2} + 4H_2O$ $E^0 = 1.5V$ [30]

Overall: $5HCOOH + 2MnO_4{}^- + 6H^+ \rightarrow 5CO_2 + 2Mn^{+2} + 4H_2O$ $E^0 = 1.75V$

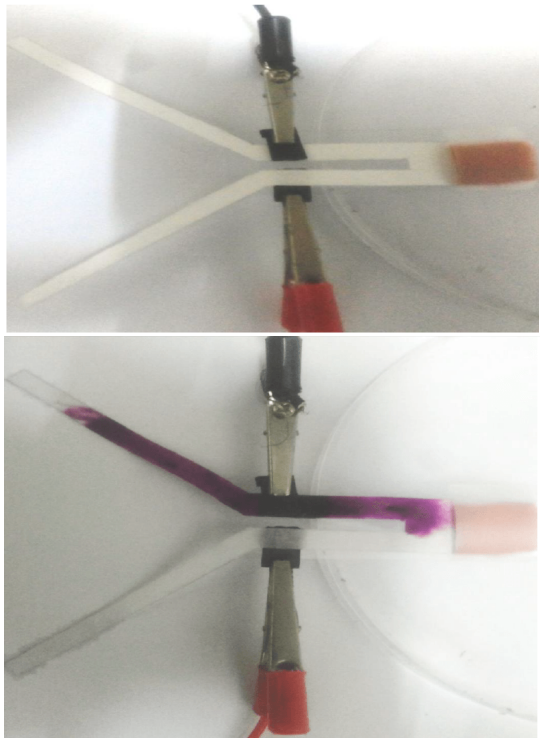

Figure 4: (a)Dry experimental cell, (b)Working cell

## 2.5 Operating conditions

The cell described here is a self-pumping cell and it works at room temperature and pressure. Only few ml of samples are enough for working of the cell. It is suggested to provide casing for the cell, so as to prevent air from entering which can add up extra undesired reactions at the electrodes. The temperature is also tried to be maintained at room temperature as the cell behaves drastically with variation in temperature.

# 3 Experimental results and discussions

## 3.1 Slit width study

- **Overview**

  The study of slit which is a unique feature present in the cell, is done with varying its width keeping the length constant at 3.5cm. As the width of the slit increases, the distance between the two electrodes increases which in return increases the ohmic losses. Also, if the slit width is decreased below a certain width, the relative mixing between the fuel and the oxidant can increase resulting in crossover losses, hence reducing the potential. So, a study on the varying width of the slit was done and an optimized slit width was determined having the highest open cell voltage(OCV) at the fuel(HCOOH) concentration of 10M and oxidant($KMnO_4$) concentration of 1M.

- **Potentiometry at various slit widths**

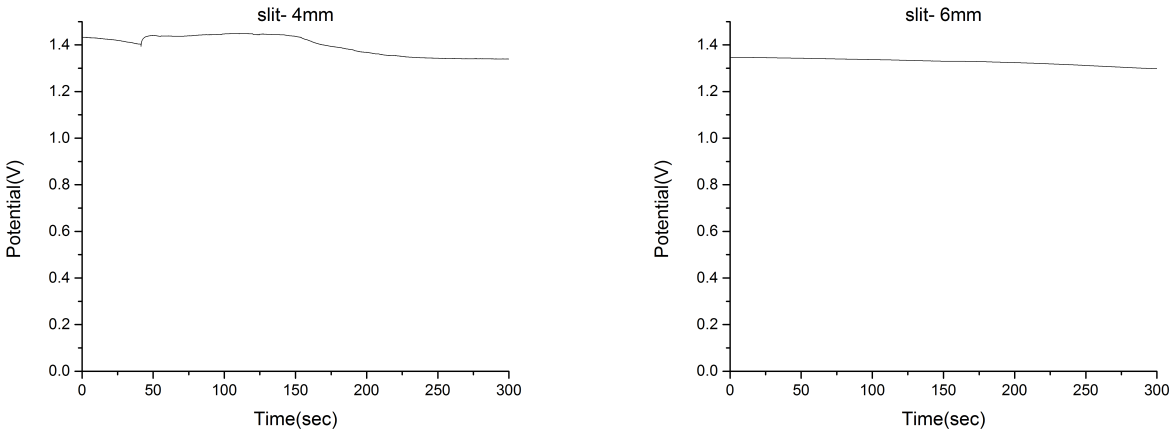


Figure 5: Potentiometric study at 1$\mu$A current for (a)slitwidth-4mm, (b)slitwidth-6mm

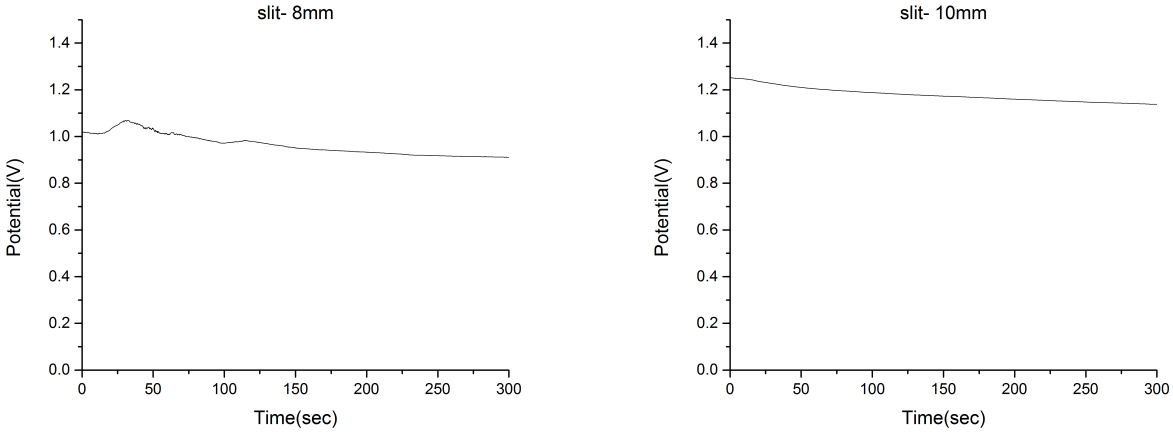


Figure 6: Potentiometric study at 1$\mu$A current for (a)slitwidth-8mm, (b)slitwidth-10mm

- **Discussion**

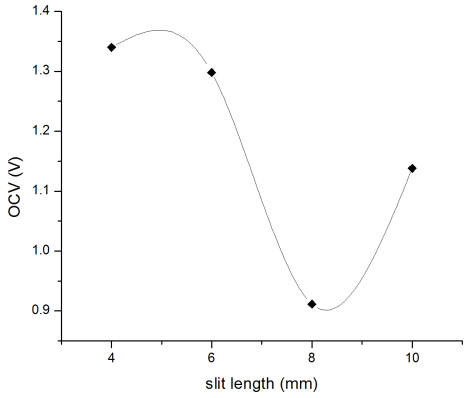


Figure 7: slit width v/s OCV

From the fig[ 5,6], it can be concluded that 4mm is the optimum slit width which gives the maximum cell voltage of 1.4V. So, slit width of 4mm can be considered as the optimized slit width. Further from fig 7, it can be attributed that initially the OCV decreases as the slit width is increased from 4mm to 6mm upto 8mm because of the increased distance

between the two electrodes, which contribute to ohmic losses. Later on at the slit width of 10mm the OCV can be seen to increase mostly due to the least crossover achieved at this width. However, we have used the slit of width 4mm for further experiments as it gives the highest OCV at the specified conditions.

## 3.2 Fuel concentration study

The fuel used in the system is the heart of the system. The cell characteristics greatly depends on the nature of the fuel. Hence, we studied the effect of concentration of the fuel(HCOOH) on the performance of the cell for various characteristic studies like potentiometry, polarization and impedance. All these studies were done at the optimum slit width of 4mm and length 3.5cm. The concentration of the fuel was varied between 6M and 12M and various characteristic curves were captured in Autolab setup as shown in coming sections. These characteristic curves decide the nature of the cell and its working efficiency in varied environments. The oxidant concentration change was also studied but as there was not much change observed, we sticked to the fuel concentration changes.

### 3.2.1 Potentiometric study

- **Overview**

  As the fuel concentration plays a vital role in the performance of the cell. A detailed analysis of variation of fuel concentration was done to look into its effects on the characteristic properties of the cell like the effective cell potential, current density, power density and FRA Impedance. So, at first the potentiometric analysis was done to measure the OCV at various concentrations of fuel, which can predict the effectiveness of the cell in terms of the deviation from the net equilibrium potential which is 1.75V for this system.

The experiment was done observing the cell voltage of the fuel cell giving a very small current of 1$\mu$A in potentiometry mode of a Autolab system. The voltage was observed for a duration of 300 seconds at each concentration. As the current applied is very low it can be considered to be the open cell voltage(OCV) of the system.

- **Results**

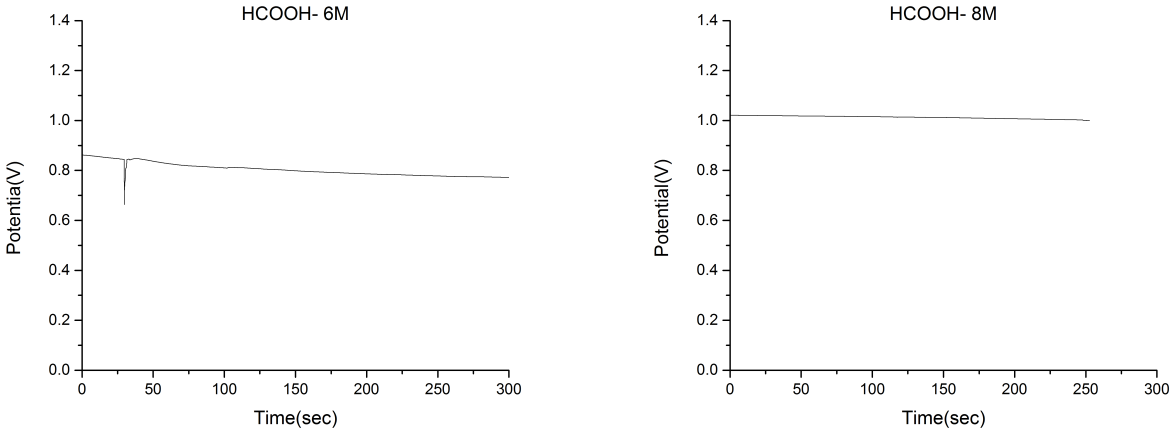


Figure 8: Potentiometric study at 1$\mu$A current for (a)HCOOH-6M, (b)HCOOH-8M

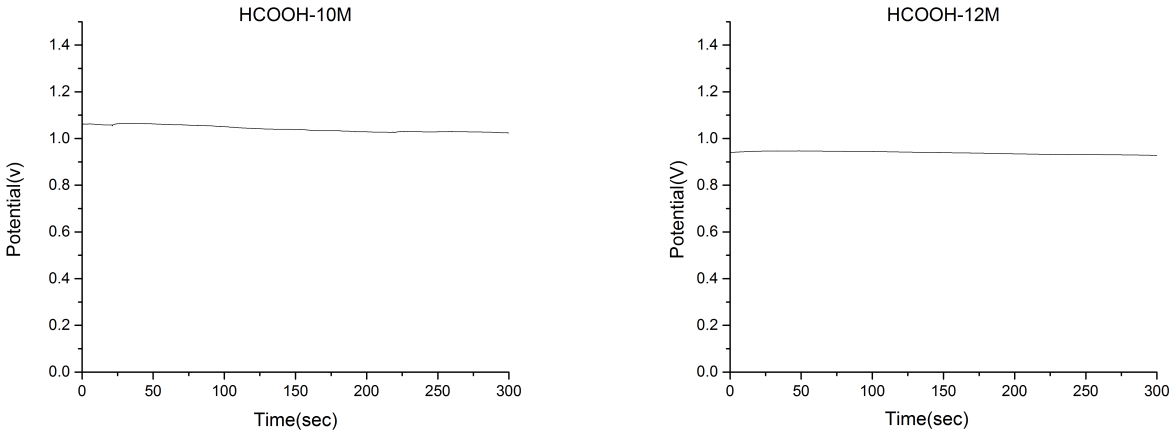


Figure 9: Potentiometric study at 1$\mu$A current for (a)HCOOH-10M, (b)HCOOH-12M

- **Discussion**

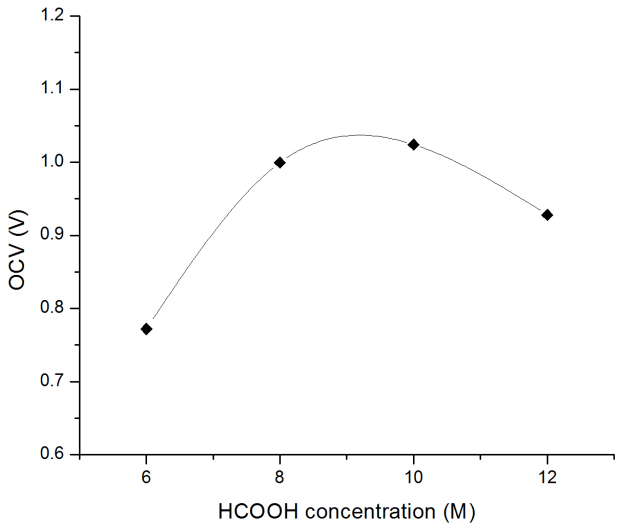


Figure 10: HCOOH concentration v/s OCV

From Fig[ 8,9], it can be concluded that 8M and 10M concentrations of fuel(HCOOH) give comparably higher value of open cell voltage(OCV) for the cell. It can be further explained by fig 10, which gives a trend of OCV varying with fuel concentration. It can be attributed that initially the OCV increases from 6M to 8M upto 10M and then falls down at later concentration of 12M. This nature of the curve can be understood as, initially as the concentration of the fuel increases, the amount of $H^+$ produced on the anode side increases, hence the transportation of protons from anode to cathode rate is higher which contributes in the increased OCV. However, after an optimum concentration of fuel the rate of anode/cathode kinetics slows down due to formation of concentration boundary layer [9]. This can further be explained as, the flow rate on the cathode side remains same in each case, whereas the concentration of fuel increases, so the cathode side reagent concentration fells short as compared to the protons reaching to it, which makes

the reaction slow hence producing low OCV after an optimum concentration of fuel. Also, the net deviation of the OCV from the equilibrium potential can be attributed to the mixed potential offered at the cathode, due to undesired reactions.[30]

### 3.2.2 Polarization curve study

- **Overview**

The polarization curve for a fuel cell is a plot between the cell voltage and the current density. Current density is an important performance variable for any fuel cell. It measures how much current can flow through a cell when load is applied to it, per unit area of the electrode. The power density is defined as the amount of power produced i.e the rate of transfer of energy per unit area by a power generating device like a fuel cell. The power density can be calculated by multiplication of the voltage applied to a cell and the current received at that voltage(VxI) or vice-versa.

Potentiometry in Autolab setup was done by giving a constant current and observing the steady cell voltage at that current. The current range starts from 1$\mu$A current which gives the OCV and goes upto the maximum current which gives zero cell voltage. Thus giving a set of cell voltage at different currents applied. The corresponding current density and the cell voltage was plotted to obtain the characteristic polarization curve for the fuel cell. Further, the corresponding power density calculated was also plotted with cell voltage in the same curve to give a better perspective of the cell performance. The similar experiments were done for all the fuel concentrations ranging from 6M to 12M.

- **Results**

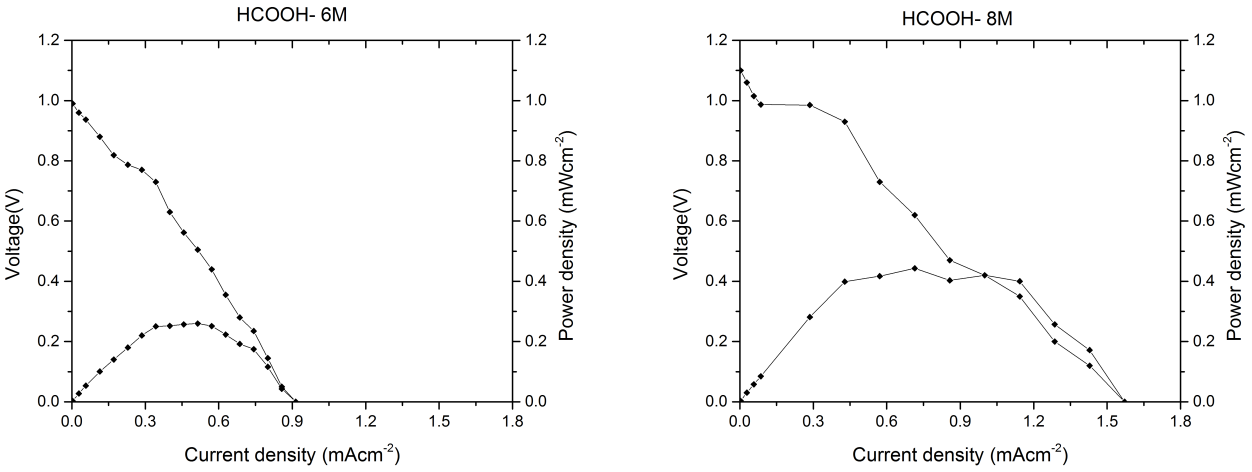


Figure 11: Polarization curve at(a)HCOOH-6M, (b)HCOOH-8M

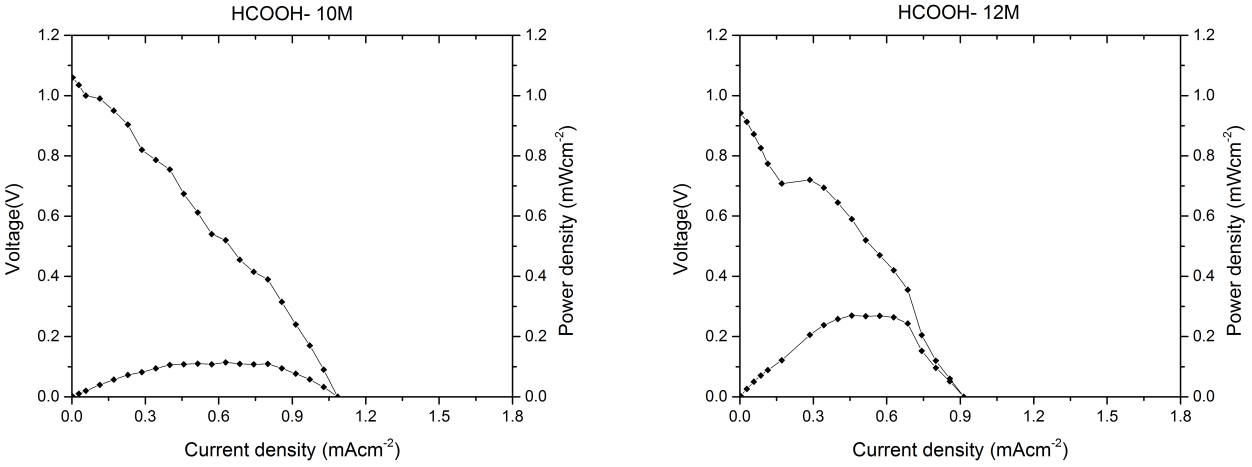


Figure 12: Polarization curve at(a)HCOOH-10M, (b)HCOOH-12M

Figure[ 11,12], depicts the characteristic polarization curve for the fuel cell. The x-intercept gives the maximum current density for the cell at a given fuel concentration. However,

the y-intercept gives the OCV for the same cell. The three different region of losses is also evident observing these curves. Also, it can be concluded that 8M concentration of fuel(HCOOH) gives highest value of current density and power density for the cell.

- **Discussion**

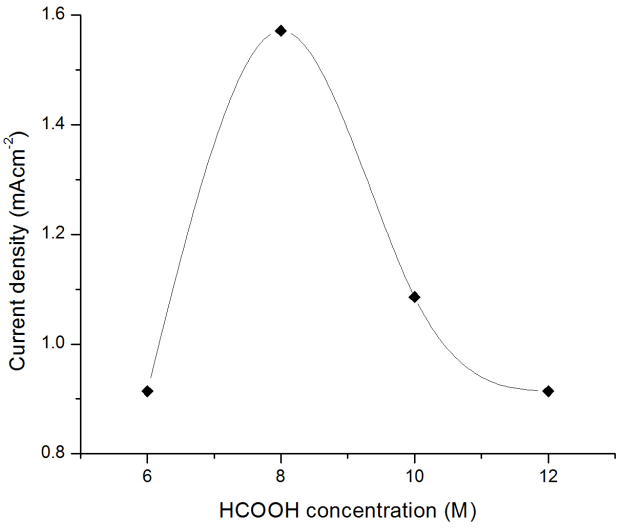


Figure 13: HCOOH concentration v/s maximum current density

Figure 13, shows a trend of variation of current density with fuel concentration. It can be observed that the current density increases from 6M to 8M gaining a maximum value of 1.57 mA/$cm^2$ and then falls down further upto 12M. The nature of this curve abides almost the same trend observed for OCV. It also supports the justification made earlier that the current density initially increases with the increase in the concentration of HCOOH due to higher transportation rate of protons from anode to cathode and gradually falls down due to consumption of the reagent at the cathode side after an optimum concentration of the fuel that can be observed to be 8M HCOOH.[16]

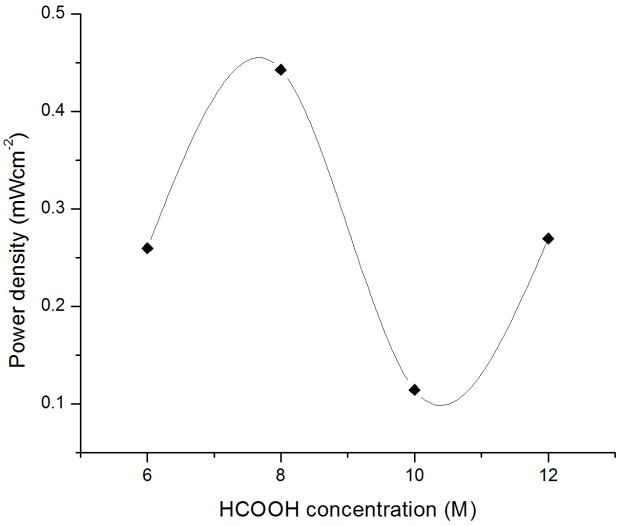


Figure 14: HCOOH concentration v/s maximum power density

Figure 14 explains the variation of maximum power density with the fuel concentration. It can be observed that the maximum power density increases from 6M to 8M reaching a maximum of 0.44 mW/$cm^2$ and then a decreasing trend is observed upto 10M. Further, a rise can be seen at 12M HCOOH concentration. This can be well explained by the net increase in $H^+$ concentration from 6M to 8M due to which the proton transfer from anode to cathode is fast leading to higher power generation. After that even though the $H^+$ concentration is still increased the poisoning of electrode surfaces occur where the microfluidic fuel cell performance is limited by slow diffusion of reagents to the electrode surface, due to the formation of concentration boundary layer. [26, 9] which leads to low power density. Further at 12M the maximum power density observed is relatively higher than that at 10M but is still lower as compared to the one observed at 8M. The current density at 12M is lower however the cell voltage is on higher side which contributes to the increased power density.

### 3.2.3 Frequency Response Analysis at various concentrations of the fuel

- **Overview**

The stability of a fuel cell can be determined by applying some perturbation to the system in terms of a sinusoidal wave of some radial frequency say, '$\omega$' and frequency 'f', where ($\omega$=2$\pi$f). The response of the system to such signals give a deterministic pathway to decide whether the system is stable or not. The method of applying such frequency to the system and analyzing its response is termed as Frequency Response Analysis(FRA).

In AC circuit the resistance is termed as Impedance(Z). The impedance possesses both magnitude and phase angle which is represented in the form of a complex number. The magnitude of the complex impedance for a sinusoidal current or voltage input is determined by the ratio of voltage amplitude to the current amplitude. The other characteristic parameter, the phase angle of the complex impedance is defined as the phase shift by which the current is ahead of voltage. The magnitude of the impedance can be shown by |Z| and the phase angle by $\theta$.[29, 8]

Nyquist plot and Bode plot are usually used to represent the impedance of the system. At every frequency the real part of the impedance (here Z') is represented in the x-axis and the imaginary part(here Z") is represented on the y-axis which forms a curve for a range of frequencies, called as Nyquist plot. In Nyquist plot exact details about frequency can not be extracted, so Bode plots are used in which the impedance is plotted with the logarithmic frequency plotted on the x-axis and both the absolute value of impedance and the phase angle are plotted on the y-axis. From, the characteristic Nyquist plots an equivalent electric circuit can be designed constituting of resistors, inductors, capacitors, diodes etc.

The few important impedance parameters which can be easily determined by observing the Nyquist plot when fitted to its equivalent electrical circuit are described as:

1. Electrolyte resistance - The resistance offered by the electrolyte while transportation of ions shares a major role in the overall impedance. This type of resistance is mainly dependent on the charge of ions and its ionic concentration in the solution. It is purely resistive in nature.

2. Double layer capacitance - The interface between electrodes and electrolyte or the interface between the two anodic and cathodic flow domains produces resistance due to the accumulation of two layers of ions with different polarities when applied a voltage across them. This type of resistance is capacitive in nature.

3. Polarization resistance - When the potential applied to a cell is forced away from its equilibrium potential or corrosion potential, the electrode is said to be polarized. This polarization of an electrode leads to flow of current due to electrochemical reactions at the electrode surface. So, the resistance offered in this case is called as polarization resistance and is purely resistive in nature. This is calculated as,

$$R_p = \Delta E / \Delta i$$

   where, $R_p$ is the polarization resistance, $\Delta E$ is variation of applied potential and $\Delta i$ is resulting polarization current.

4. Charge transfer resistance - For a single kinetically controlled electrochemical reaction, the resistance offered is similar to polarization resistance which is termed as charge transfer resistance. In this case there is mixed potential, but only a single reaction is at equilibrium.

Charge transfer is the transfer of electron from the ionic species in the solution to the solid metal which basically produces the resistance.

5. Diffusion resistance - As diffusion is very important in this kind of systems. The diffusion of fuel to the electrodes and the back diffusion of ions from electrodes to the electrolyte, diffusion resistances occurs, which can be shown by elements like Warburg element for semi-infinite linear diffusion and by O, T, G elements for finite diffusional lengths.[10]

- **Nyquist plots at different concentrations of fuel**

The signal used for measuring the FRA impedance was taken as sine waves with amplitude of 0.01V and frequency was varied from 1MHz to 0.1Hz for which corresponding impedance curves were plotted.

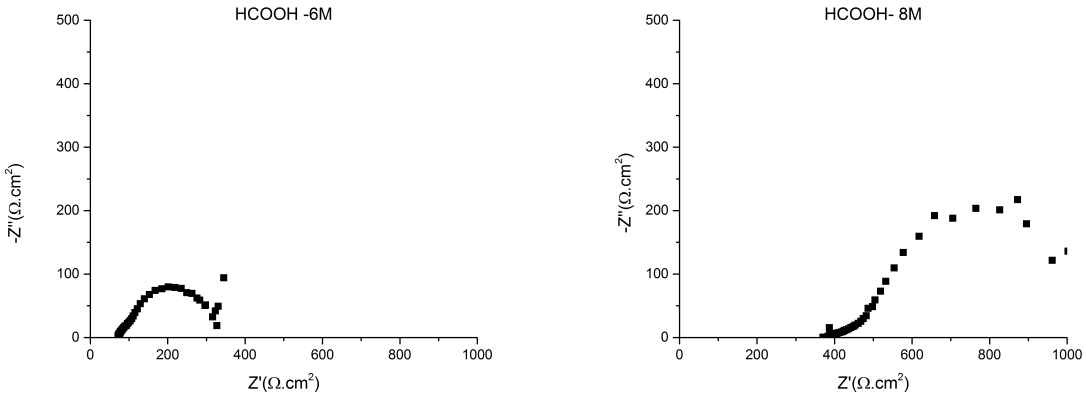


Figure 15: Nyquist plots at(a)HCOOH-6M, (b)HCOOH-8M

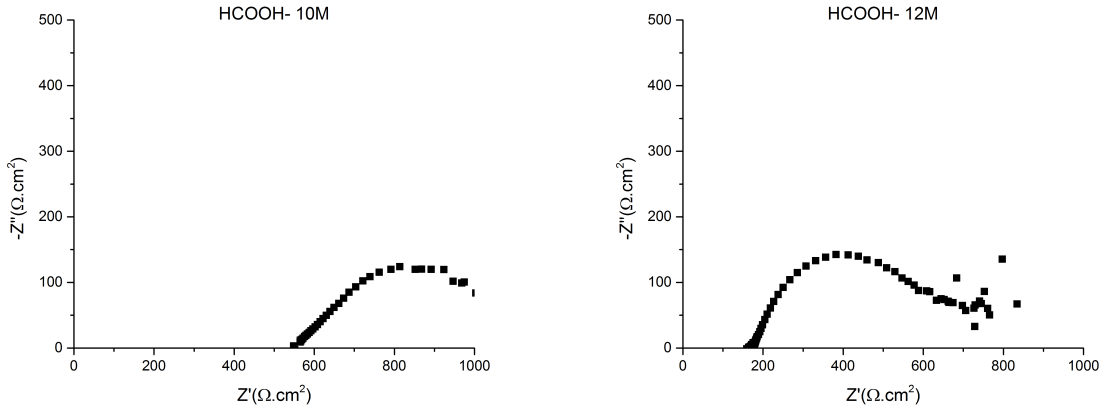


Figure 16: Nyquist plots at(a)HCOOH-10M, (b)HCOOH-12M

The Nyquist plot shown in Fig[ 15,16],shows the behavior of the cell when a perturbation in terms of sine wave signals are fed to the system. The plot above shows that the cell resembles to a 'Randles circuit' more likely as it tries to form almost a semicircular arc in each case. The initial intercept of the curve on the x-axis gives the solution resistance ($R_s$) , which is the resistance offered mostly by the electrolyte. The intercept on the x-axis at the end of the semicircular arc is the sum of the solution resistance ($R_s$) and the charge transfer resistance ($R_{ct}$).

It can be observed that the solution resistance increases from 6M upto 10M and then reduces at 12M. In our system, fuel and electrolyte are mixed together, so as the fuel concentration is increased without varying the electrolyte concentration, the overall electrolyte concentration in the mixture decreases. So, as the fuel concentration increases upto 10M the overall electrolyte concentration is reduced i.e the mobility of $H^+$ ion is decreased which in turn offers resistance. However, as further concentration of fuel is increased, the amount of $H^+$ in the solution increases to a large extent which is self sufficient to maintain flow from anode side to cathode side, so even though the electrolyte concentration present in the system is low, the mobility of protons is high enough and hence the overall solution resistance is on lower side.

- **Bode phase plots at different concentrations of fuel**

The bode phase plot of phase angle($\phi$) versus log$\omega$ was studied based on the FRA curves obtained as shown in Fig[ 17,18].The Nyquist plot as shown above is not able to give idea about variations at a particular frequency or $\omega$. So, bode plots are studied. These also gives a hands on knowledge about the nature of the equivalent electrical circuit without proper fit. The typical nature of humps, as can be seen in the bode plot at middle value frequencies suggests about the equivalent circuit with a resistance in series with a constant phase element and an another resistance in parallel to it, which resembles to a 'Randels circuit' as can be noticed from the Nyquist plot. The disturbances at lower frequencies can be attributed to some diffusional resistances in the circuit, but is not fully confined as can be seen in the curves.[23]

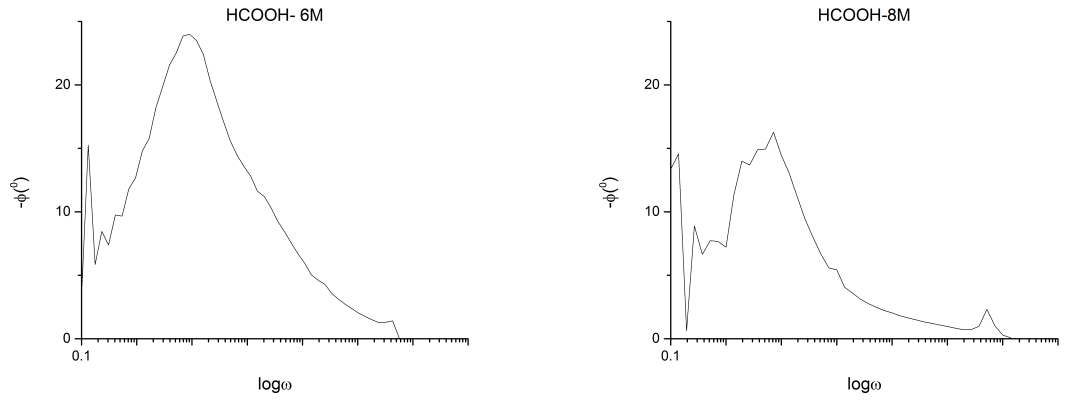


Figure 17: Bode phase plots at(a)HCOOH-6M, (b)HCOOH-8M

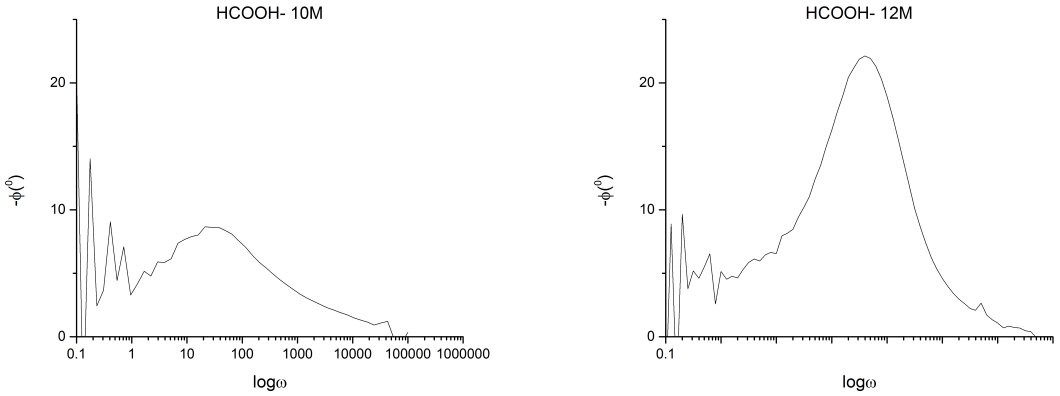


Figure 18: Bode phase plots at(a)HCOOH-10M, (b)HCOOH-12M

- **Bode modulus plots at different concentrations of fuel**

The bode modulus plot of impedance(Z) versus log$\omega$ was studied based on the FRA curves obtained as shown in Fig[ 19,20]. It shows the net impedance value at various $\omega$, which can not be obtained from the Nyquist plot. At lower frequency, the net impedance is increased due to resistances added by diffusional, polarization resistances coming into picture. However, at higher frequencies only the solution resistance plays significant role which can be seen as a constant line at the end in these plots. The various resistances shown in Nyquist plot can be verified here.

At all the concentrations, the initial starting of the bode modulus curve shows some fluctuations at lower values of frequency, which can be attributed to the extra diffusional resistance. In 12M HCOOH, the fluctuations are higher, so diffusional resistance can be assumed to be highest among all. The Bode modulus curve well supports the assumptions made from the Nyquist plot and the Bode phase plot, which can combinely explains the nature of the cell.

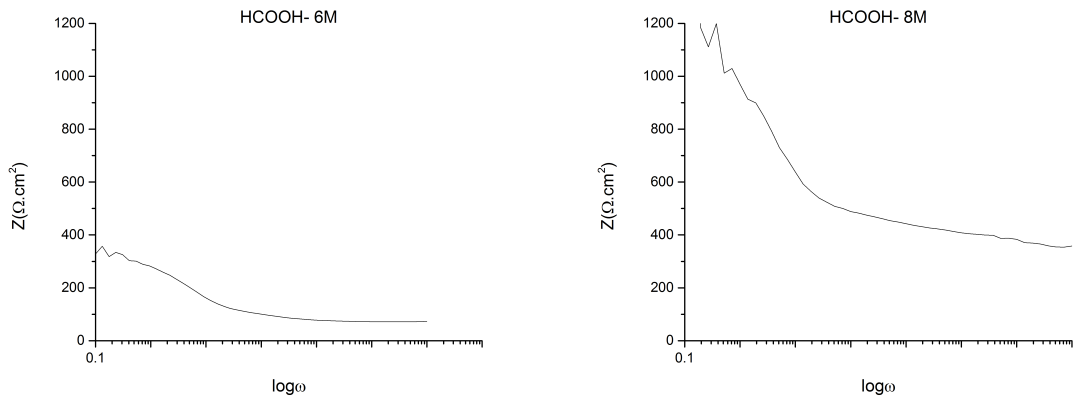


Figure 19: Bode modulus plots at(a)HCOOH-6M, (b)HCOOH-8M

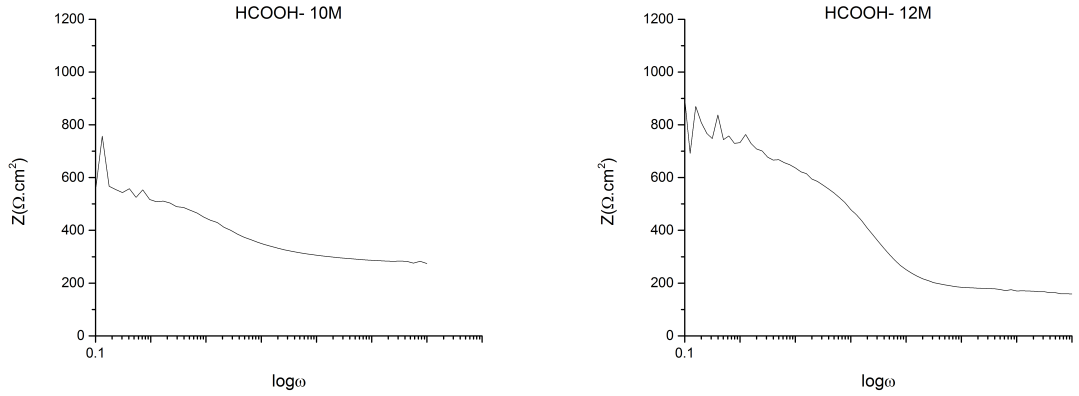


Figure 20: Bode modulus plots at(a)HCOOH-10M, (b)HCOOH-12M

# 4 Conclusion and Future scope

## 4.1 Conclusion

In this work, a paper fuel cell has been fabricated, which is designed to be used as a cost effective, portable, green energy source. Here, whatman filter paper has been used as the media for flow of fuel, oxidant, electrolyte and ions between the electrodes shaped in a Y-structure. The capillary action on the paper allows the fuel and oxidant to pump on it without any extra power source, hence it is called self-pumping. HCOOH has been used as fuel, as it can be operated at room temperature. 1M $KMnO_4$ is used as oxidant in place of conventional $O_2$ to gain higher OCV. A unique kind of modification was done in the system by providing a slit at the entrance of the cell, which helps in reducing mixing and hence crossover. The slit length was optimized by studying the OCV values at different slit widths using potentiometry at a fixed slit length of 3.5cm. The optimized slit width was found to be 4mm. The further studies were done at this optimized slit width varying concentrations of HCOOH and parameters like OCV, current density, power density, Impedance of the cell were observed. The concentration of HCOOH was varied from 6M, 8M, 10M to 12M. The maximum OCV of 1.02V was obtained at the concentration of 10M which is comparable to 0.99V observed at 8M HCOOH. The maximum current density of 1.57mA$cm^{-2}$ was also observed at the same concentration of 8M. The power density at this concentration was 0.44mW$cm^{-2}$, which was again highest among all other concentrations. So, 8M of HCOOH can be assumed to be the optimized concentration of the fuel for this system. The observed amount of current density and power density is well suited for small diagnostic devices application of the cell. The amount of fuel, oxidant and electrolyte being used is very small and hence make the device cost-effective. The electrodes used is plain graphite and no catalyst has been used, separate current collector is also not required as graphite is itself conducting, so it makes the system overall more cost savior. Hence, it can be concluded that the system can be used for

small scale devices with low power consumption.

## 4.2 Future scope

The current density of the cell can be further tried to be improved by using suitable catalysts on the electrode surface based on the study of kinetics of the reactions at electrodes. The Nyquist plot obtained by FRA impedance for various concentrations can be used to fit the equivalent electrical circuit in terms of various electrical components, which can well explain the characteristic losses occurring in the cell. The design of the cell can be further improved by using solidified form of fuel and oxidant in the form of cartridges. In addition, studies can be done to tackle the issues that leads to deviation from the equilibrium potential and steps can be taken to minimize them. Overall, there is a wide scope of making the cell more robust and efficient.

# References


[1] Ravi Kumar Arun, Saurav Halder, Nripen Chanda, and Suman Chakraborty. Lab on a chip communication a paper based self-pumping and self-breathing fuel cell using pencil stroked graphite electrodes. 14, 2014.

[2] William A Braff, Martin Z Bazant, and Cullen R Buie. Membrane-less hydrogen bromine flow battery. *Nature communications*, 4, 2013.

[3] Fikile R Brushett, Ranga S Jayashree, Wei-Ping Zhou, and Paul JA Kenis. Investigation of fuel and media flexible laminar flow-based fuel cells. *Electrochimica Acta*, 54(27):7099–7105, 2009.

[4] Min-Hsing Chang, Falin Chen, and Nai-Siang Fang. Analysis of membraneless fuel cell using laminar flow in a y-shaped microchannel. *Journal of Power Sources*, 159(2):810–816, 2006.

[5] E Choban. Microfluidic fuel cell based on laminar flow, 2004.

[6] Eric R Choban, Larry J Markoski, Andrzej Wieckowski, and Paul JA Kenis. Microfluidic fuel cell based on laminar flow. *Journal of Power Sources*, 128(1):54–60, 2004.

[7] Eric R Choban, JS Spendelow, L Gancs, A Wieckowski, and PJA Kenis. Membraneless laminar flow-based micro fuel cells operating in alkaline, acidic, and acidic/alkaline media. *Electrochimica Acta*, 50(27):5390–5398, 2005.

[8] K. R. Cooper and M. Smith. Electrical test methods for on-line fuel cell ohmic resistance measurement. *Journal of Power Sources*, 2006.

[9] A. Déctor, J. P. Esquivel, M. J. González, M. Guerra-Balcázar, J. Ledesma-García, N. Sabaté, and L. G. Arriaga. Formic acid microfluidic fuel cell evaluation in different oxidant conditions. *Electrochimica Acta*, 2013.

[10] Inc. EG&G Technical Services. *Fuel Cell Handbook*. 2004.

[11] J P Esquivel, F J Del Campo, J L Omez De La Fuente, S Rojas, and N Saba. Microfluidic fuel cells on paper: meeting the power needs of next generation lateral flow devices.

[12] Rosaria Ferrigno, Abraham D. Stroock, Thomas D. Clark, Michael Mayer, and George M. Whitesides. Membraneless vanadium redox fuel cell using laminar flow. *Journal of the American Chemical Society*, 2002.

[13] Arwa Fraiwan, Sayantika Mukherjee, Steven Sundermier, Hyung Sool Lee, and Seokheun Choi. A paper-based microbial fuel cell: Instant battery for disposable diagnostic devices. *Biosensors and Bioelectronics*, 2013.

[14] Rafael Abraham García-Cuevas, Ilse Cervantes, Luis Gerardo Arriaga, and Irwin Allen Diaz-Diaz. Toward geometrical design improvement of membraneless fuel cells: Numerical study. *International Journal of Hydrogen Energy*, 38(34):14791–14800, 2013.

[15] Seung-Mo Ha and Yoomin Ahn. Laminar flow-based micro fuel cell utilizing grooved electrode surface. *Journal of Power Sources*, 267:731–738, 2014.

[16] Ping Hong, Shijun Liao, Jianhuang Zeng, and Xinjian Huang. Design, fabrication and performance evaluation of a miniature air breathing direct formic acid fuel cell based on printed circuit board technology. *Journal of Power Sources*, 2010.

[17] Ping Hong, Fan Luo, Shijun Liao, and Jianhuang Zeng. Effects of pt/c, pd/c and pdpt/c anode catalysts on the performance and stability of air breathing direct formic acid fuel cells. *International Journal of Hydrogen Energy*, 36(14):8518–8524, 2011.

[18] Ranga S. Jayashree, Lajos Gancs, Eric R. Choban, Alex Primak, Dilip Natarajan, Larry J. Markoski, and P. J A Kenis. Air-breathing laminar low-based microfluidic fuel cell. *Journal of the American Chemical Society*, 2005.

[19] Ranga S Jayashree, Seong Kee Yoon, Fikile R Brushett, Pedro O Lopez-Montesinos, Dilip Natarajan, Larry J Markoski, and Paul JA Kenis. On the performance of membraneless laminar flow-based fuel cells. *Journal of Power Sources*, 195(11):3569–3578, 2010.

[20] Fikile R. Brushett; Ranga S. Jayashree; Wei-Ping Zhou; Paul J.A. Kenis. Investigation of fuel and media flexible laminar flow-based fuel cells. *Electrochimica Acta*, 54, 2009.

[21] Erik Kjeang, Alexandre G Brolo, David A Harrington, Ned Djilali, and David Sinton. Hydrogen peroxide as an oxidant for microfluidic fuel cells. *Journal of the Electrochemical Society*, 154(12):B1220–B1226, 2007.

[22] Erik Kjeang, Raphaelle Michel, David A Harrington, Ned Djilali, and David Sinton. A microfluidic fuel cell with flow-through porous electrodes. *Journal of the American Chemical Society*, 130(12):4000–4006, 2008.

[23] Andrzej Lasia. Electrochemical impedance spectroscopy and its applications. In *Modern aspects of electrochemistry*, pages 143–248. Springer, 2002.

[24] P. O. López-Montesinos, N. Yossakda, A. Schmidt, F. R. Brushett, W. E. Pelton, and P. J A Kenis. Design, fabrication, and characterization of a planar, silicon-based, monolithically integrated micro laminar flow fuel cell with a bridge-shaped microchannel cross-section. *Journal of Power Sources*, 2011.

[25] D Morales-Acosta, MD Morales-Acosta, LA Godinez, L Alvarez-Contreras, SM Duron-Torres, J Ledesma-Garcia, and LG Arriaga. Pdco supported on multiwalled carbon nanotubes as an anode catalyst in a microfluidic formic acid fuel cell. *Journal of Power Sources*, 196(22):9270–9275, 2011.

[26] D. Morales-Acosta, H. Rodríguez G., Luis A. Godinez, and L. G. Arriaga. Performance increase of microfluidic formic acid fuel cell using pd/mwcnts as catalyst. *Journal of Power Sources*, 2010.

[27] Nicolas Da Mota, David A Finkelstein, Joseph D Kirtland, Claudia A Rodriguez, Abraham D Stroock, and Hector D Abruna. Membraneless, room-temperature, direct borohydride/cerium fuel cell with power density of over 0.25 w/cm2. *Journal of the American Chemical Society*, 134(14):6076–6079, 2012.

[28] Hong Beom Park, Dewan Hasan Ahmed, Kyung Heon Lee, and Hyung Jin Sung. An h-shaped design for membraneless micro fuel cells. *Electrochimica Acta*, 54(18):4416–4425, 2009.

[29] Ramaraja P Ramaswamy, Narendran Sekar, and Ramaraja P Ramasamy. Microbial & biochemical technology electrochemical impedance spectroscopy for microbial fuel cell characterization. *J Microbial Biochem Technol J Microb Biochem Technol*, 6, 2013.

[30] Kamil S. Salloum, Joel R. Hayes, Cody A. Friesen, and Jonathan D. Posner. Sequential flow membraneless microfluidic fuel cell with porous electrodes. *Journal of Power Sources*, 2008.

[31] M.H. Sun, G. Velve Casquillas, S.S. Guo, J. Shi, H. Ji, Q. Ouyang, and Y. Chen. Characterization of microfluidic fuel cell based on multiple laminar flow, 2007.

[32] Xingwen Yu and Peter G. Pickup. Recent advances in direct formic acid fuel cells (dfafc), 2008.